Designing for Cavitation-Free Operation on Hydrofoils with NACA 16-Series Sections

ALAN C. CONOLLY*
General Dynamics, San Diego, Calif.

The necessity for designing for cavitation-free operation on a proposed subcavitating hydrofoil craft has led to considerable research effort into the study of hydrofoil cavitation. Six NACA 16-series foil sections were investigated theoretically by a method developed at the Bureau of Ships to obtain cavitation boundaries for a three-dimensional foil-pod system. In order to carry out a more complete parametric study quickly, two-dimensional cavitation buckets for these six NACA 16-series sections developed by the Abbott method for obtaining pressure distributions have been factored to collapse onto the buckets obtained by detailed calculations. With the factors obtained, a large number of sections were evaluated for a cruising depth of 2.5 ft, and a foil selection chart has been developed. Hydrofoil section NACA 16-407 was selected for both main and stern foils on the proposed craft after considering the relationships between foil loading and hydrodynamic drag, and also C_L range, uncavitated, within the bucket, and rough-water performance and turning characteristics. To make this chart usable for the preliminary design of other hydrofoil craft, the effects of foil depth of immersion, sweep, and taper ratio on the cavitation buckets have been briefly investigated.

Nomenclature

C_L	=	hydrofoil lift coefficient
C_D	=	hydrofoil drag coefficient
A	=	aspect ratio
t	=	maximum hydrofoil thickness
c	=	hydrofoil chord
α	=	angle of foil incidence
$C_{L\alpha}$	=	three-dimensional lift curve slope per degree
$C_{L\alpha\ \exp}$	=	two-dimensional lift curve slope per radian
ρ	=	density of water, lb-sec^2/ft^4
V	=	craft velocity, fps
S	=	foil area, ft^2
W	=	weight of craft, lb
$\alpha_{L=0}$	=	angle of zero lift for foil section
V_C	=	incipient cavitation velocity, fps
C_{PU}	=	pressure coefficient at a point on the hydrofoil's upper surface
C_{PL}	=	pressure coefficient at a point on the hydrofoil's lower surface
Δp	=	pressure difference, psf
q	=	dynamic pressure ($\frac{1}{2}\rho V^2$)
v/V, $\Delta v/V_a$ $\Delta v_a/V$	=	pressure distributions due, respectively, to zero-camber thickness at zero angle of attack, the addition due to the cambered mean line, and the additional distribution associated with angle of attack
p_∞	=	ambient pressure at foil depth, psf
p_v	=	vapor pressure of water, psf
Λ	=	sweep angle of foil $\frac{1}{4}$ chord line
σ_v	=	cavitation number based on vapor pressure

Introduction

THE Bureau of Ships gave General Dynamics guidance as to a feasiblity design for a set of subcavitating hydrofoils and struts to be fitted to the U. S. Navy "Fresh I" research craft. It was stipulated that the design should be for an airplane foil configuration with 80% of the load on the forward foils and 20% on the aft foil. All three struts, which would house experimental hydrofoil stabilization units known as Hystad, were to be of the same size. The rear strut was to be steerable. The forward struts were to be NACA 16-series, which are very suitable for hydrofoils and on which there is a wealth of design data. The foil planforms were stipulated, and the pods at the foil-strut intersections were to be developed from the D.T.M.B. series 58 underwater bodies. Their size was dictated by the design of the pivot for the fully incidence-controlled hydrofoils.

The craft was to be able to cruise at 45 knots in smooth water and up to a sea-state 3 without cavitation. A drawing of the "Fresh I" fitted with the general Dynamics foil system is shown in Fig. 1 and a drawing of the main foil-pod-strut in Fig. 2.

A model test program[1] was carried out in the General Dynamics/Electric Boat Towing Basin, paralleling the hydrodynamic and structural design, to provide data for calculating stability derivatives. A separate test program[2] with the same model foils was performed at the D.T.M.B. Towing Basin at Langley Field, Va., to check on the cavitation characteristics.

Although a great deal is known about the low-speed characteristics of subcavitating hydrofoils, only recently has much work been done on accurate prediction of cavitation and its effect on a three-dimensional strut-foil system. Papers by Johnson,[3] Brockett,[4] and Bauman[5] show how to design for cavitation-free operation at a desired lift coefficient and speed for a given foil configuration, but the method is complicated and is still not backed up by sufficient experimental data.

Because of the complexities of this part of the design and the problems connected with choosing a suitable foil section, even after this has been defined as NACA 16-series, the present paper will concentrate on this particular aspect of the hydrodynamic design.

Designing for Cavitation-Free Operation

There are three technical reasons why the craft should be designed for, as nearly as possible, cavitation-free operation:

1) Cavitation on a subcavitating section causes erosion (by the shock waves created by imploding cavitation bubbles), corrosion (accelerated by the spoiling of the smooth surface by

Presented as Preprint 65-449 at the AIAA Second Annual Meeting, San Francisco, Calif., July 26–29, 1965; submitted August 9, 1965; revision received April 18, 1966. The opinions expressed in this paper are strictly those of the author and do not necessarily reflect the views of either the Bureau of Ships or General Dynamics, Electric Boat Division. The author is indebted for the assistance given by the U. S. Navy Bureau of Ships.

* Senior Hydrodynamic, Engineers Electric Boat Division, Marine Technology Center.

erosion), and vibration (because of unsteady flow conditions). The destruction of the accurately machined surface causes cavitation to occur even earlier and starts a vicious cycle of events.

2) If sheet cavitation were to occur on the upper surface of a foil, say during a turn, then there would be a loss of lift on the foil. The control system would call for an increased angle of incidence and would only aggravate the condition.

3) Not very much is known of the falloff in lift after the occurrence of incipient cavitation.

However, because of the excessive power of the engine on the "Fresh I" and the temptation to try a little more speed, it is fairly certain that cavitation will occur in "off-design" operation, and therefore it is necessary to know what are the cavitation boundaries and what will happen when these boundaries are *exceeded*.

With regard to the incipient cavitation boundaries themselves, these are usually represented by a bucket-shaped envelope on a graph with vertical and horizontal abscissa of lift coefficient and cavitation number or speed in knots, respectively. The bucket is directly a function of the geometry of the hydrofoil and the C_L developed, which is also dependent on such items as aspect ratio, sweep, taper, and depth in the water. For the two-dimensional foil, the bucket position and shape are mainly controlled by the camber and foil thickness. Increasing camber moves the bucket upward on C_L, the bottom of the bucket to a lower speed, and decreases the width of the bucket. Increasing foil thickness does not change the C_L location of the bucket appreciably but lowers the speed of the bottom of the bucket and widens the C_L range of the bucket.

Two-dimensional cavitation buckets can be calculated by the Abbott[6] method, and this calculation and an illustration of the effects of camber and thickness are given later in this paper. The Bureau of Ships has written a computer program in Fortran II for the IBM 1620 machine for performing this calculation, and so a large number of foil sections can be easily compared.

Unfortunately, the two-dimensional bucket does not give the three-dimensional cavitation characteristics, which is the reason for the paper by Johnson.[3] It is costly and time-consuming to analyze a large number of sections by Johnson's method, and yet a design chart is urgently needed for preliminary foil design of a projected hydrofoil boat. It can be fairly approximate, and then the section or sections chosen can be analyzed in more detail.

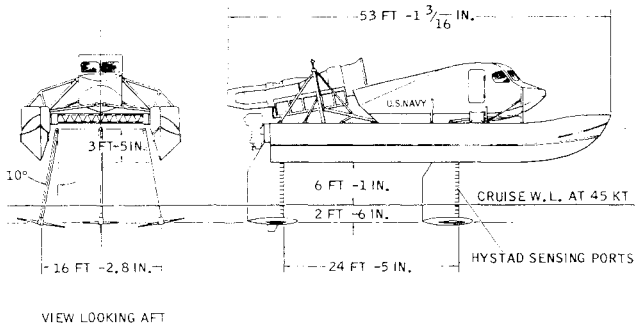

DESIGN CRAFT GROSS WT 41,500 LB

	MAIN FOIL	STERN FOIL
FOIL AREA - SQ. FT	15.24	7.62
ASPECT RATIO	3.0	3.0
TAPER RATIO	0.3	0.3
FOIL SECTION NORM. TO 1/4 CHORD	NACA 16 - 407	
DESIGN C_L	0.40	0.40
a	1.0	1.0
SWEEP 1/4 CHORD LINE	35.2°	35.2°
STRUT SECTION	NACA - 16 - 010	

Fig. 1 U. S. Navy "Fresh I" fitted with "Hystad" subcavitating foils.

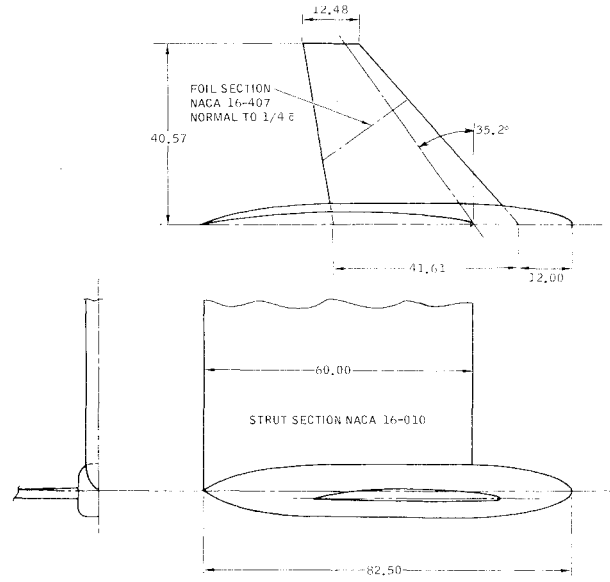

Fig. 2 Subcavitating hydrofoil (Hystad): main foil-pod-strut.

Development of a Foil Selection Chart

Let us assume that the designer has been given the foil section as NACA 16-series and that he has decided upon preliminary craft gross weight, foil area, aspect ratio, sweep, taper, operating depth, design speed, sea-states, trimming requirements, operational speed, and maximum speed. Most of these items will be decided fairly early in a project.

He will know what C_L he requires at his operational speed and what range of C_L, without cavitation, he requires at this speed for sea-states and craft turns. It was decided that, in developing a foil selection chart, the three-dimensional cavitation bucket can be defined as follows:

1) C_L required at operational speed, which will be made to bisect the bucket width at this speed. This C_L is a function of foil loading.

2) The C_L range, uncavitated, at the operational speed, i.e., the width of the bucket at this speed.

3) The absolute maximum speed without cavitation, i.e., the bottom right-hand corner of the bucket. (The craft operating line will normally come close to this point.)

These definitions are illustrated in Fig. 3. Six sections, defined normal to the foil $\frac{1}{4}$ chord line, were analyzed by the

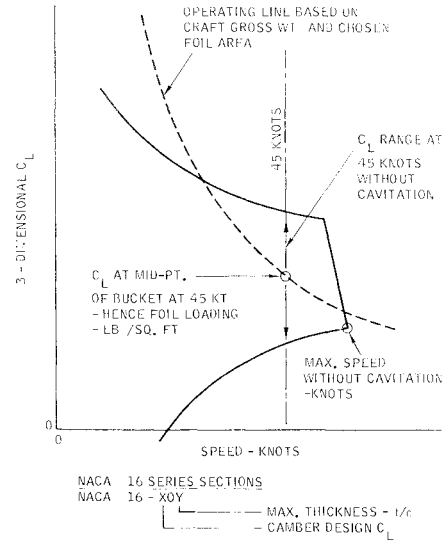

Fig. 3 Definitions for foil selection chart.

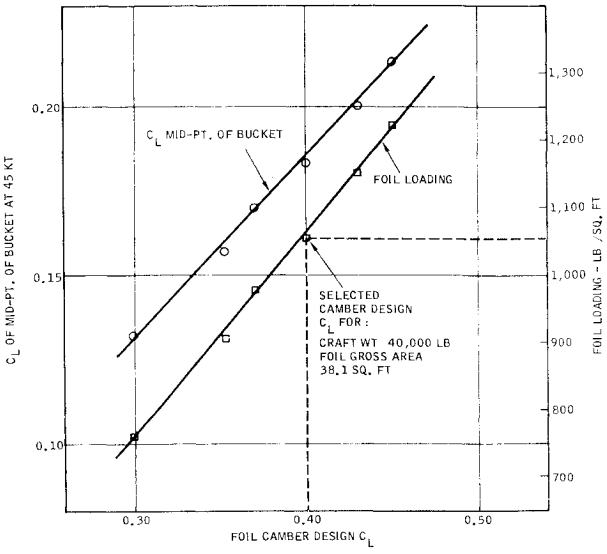

Fig. 4 Three-dimensional foils evaluated for the "HYSTAD" boat.

BuShips method for the Hystad craft. These were NACA-16-308, NACA-16-353/08, NACA-16-37/073, NACA-16-407, NACA-16-43/07, and NACA-16-45/067. They were all chosen to give a maximum noncavitating speed of about 52 knots at a foil depth of 2.5 ft. They cover a range of foil loading from 760 to 1225 psf for a range of C_L at the midpoint of the bucket at 45 knots from 0.132 to 0.213, respectively. This is illustrated in Fig. 4. This is a good range of sections at one design speed and gives the basis for a selection chart.

A quick method was required for approximating the three-dimensional buckets that were obtained from the results of the BuShips computer programs. The approach adopted was to take the NACA 16-series sections defined streamwise, to calculate the Abbott bucket[6] (two-dimensional unswept), multiply the C_L's by a constant factor, and then add a second constant to these resultant C_L's. A third constant was then added to all values of critical speed. By this means, a very close approximation was made to the three-dimensional

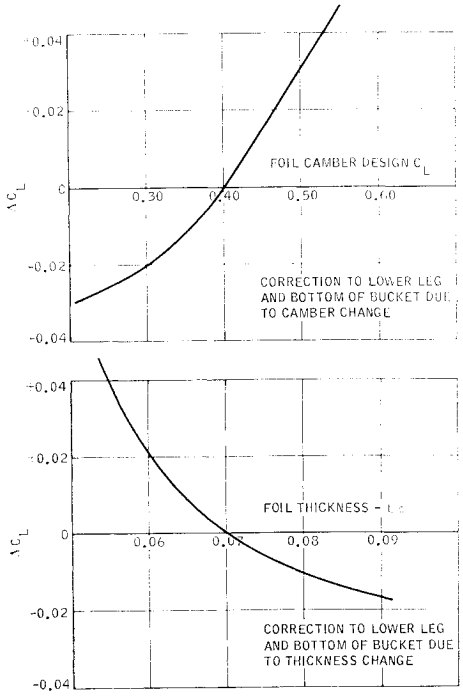

Fig. 5 Final C_L corrections for camber and thickness.

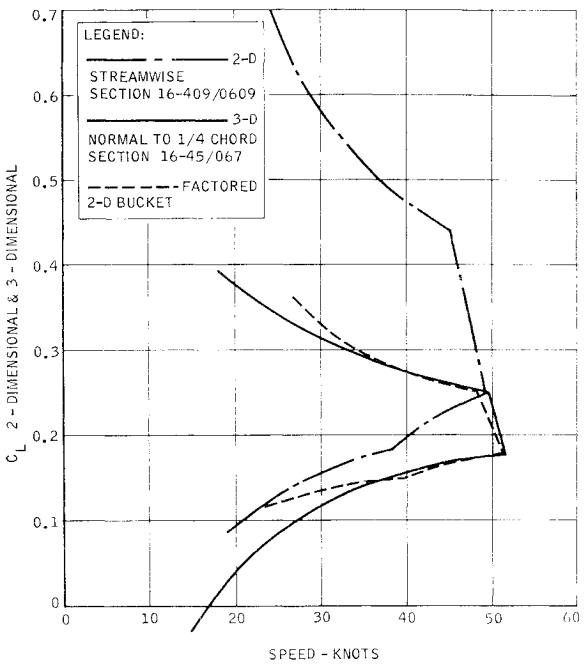

Fig. 6 Corrections to Abbott two-dimensional cavitation bucket.

NACA 16-407 cavitation bucket. This section was then used as a datum point. The other sections just listed were then approximated very closely by a further camber correction and a thickness correction from Fig. 5. This is an arbitrary, engineer's approach to the problem but one that works for a first stab at the foil section.

Figure 6 shows the effect of applying these factors to the two-dimensional cavitation bucket for the NACA 16-409/0609 section. This is the approximate NACA streamwise section for the tapered HYSTAD foil with a normal to

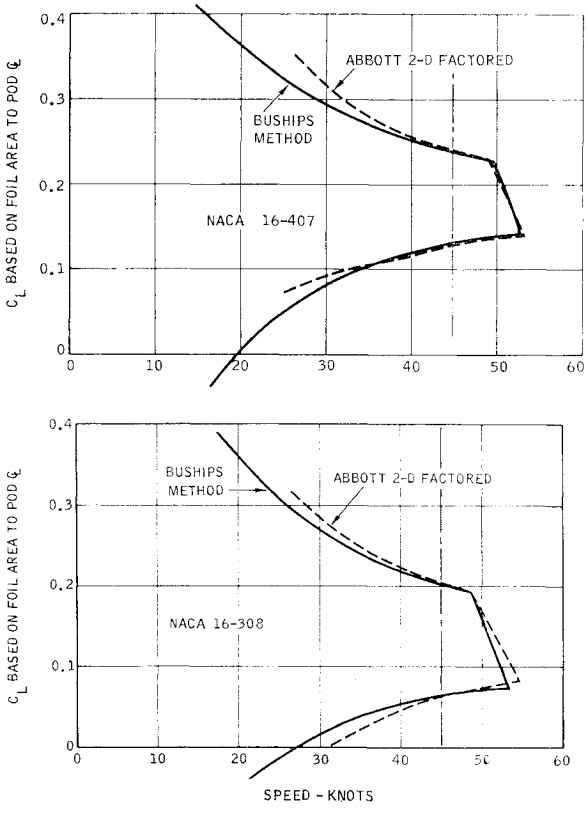

Fig. 7 Factoring of two-dimensional cavitation buckets.

Table 1 Abbott two-dimensional cavitation data with factoring[a]

Surface	Location x/c, %	① 2-D crit. speed, knots	② 3-D crit. speed, knots, = ① + 2.5	③ 2-D C_L	④ 2-D $C_L \times 0.45$	⑤ 3-D C_L = ④ + 0.05	⑥ 3-D C_L = ⑤ − 0.03
Bottom	1.25	33.9	36.4	0.023	0.010	...	0.030
Bottom	1.25	36.2	38.7	0.048	0.022	...	0.042
Bottom	1.25	39.1	41.6	0.073	0.033	...	0.053
Bottom	1.25	42.7	45.2	0.098	0.044	...	0.064
Top	60.0	51.9	54.4	0.148	0.067	...	0.087
Top	60.0	50.6	53.1	0.198	0.089	...	0.109
Top	60.0	49.5	52.0	0.248	0.112	...	0.132
Top	60.0	48.3	50.8	0.298	0.134	...	0.154
Top	1.25	42.6	45.1	0.348	0.157	0.207	...
Top	1.25	39.0	41.5	0.373	0.168	0.218	...
Top	1.25	36.2	38.7	0.398	0.179	0.229	...

[a] Section NACA 16-308 normal to ¼ chord; section NACA 16-273/0727 streamwise. From RSJ/080 program for streamwise section NACA 16-series with an a = 1.0 mean line. Sweep = 0.00°, depth = 2.50 ft. C_L corrections fro m Fig. 5 (camber correction, −0.020; thickness correction, −0.010; total, −0.030).

¼ chord section of NACA 16-45/067. The agreement between the factored Abbott bucket and the bucket obtained by the BuShips three-dimensional analysis is shown to be very close in the speed region of interest. Table 1 gives the two-dimensional results for a streamwise section of NACA 16-273/0727 (normal to ¼ chord section NACA 16-308) with three-dimensionalizing factors applied.

Figure 7 shows the collapse obtained to the three-dimensional cavitation buckets for the normal to ¼ chord sections NACA 16-407 and NACA 16-308. In Fig. 8, families of corrected cavitation buckets have been plotted for foil thicknesses of 7 and 8% defined normal to the ¼ chord. This figure indicates that two-dimensional calculations do show the effects of variation in foil thickness and camber on cavitation speed but give absolute values that are incorrect unless factored. Using these plots for a large range of foil sections and with the definitions in Fig. 3, cross-plots were made which enabled the foil selection chart of Fig. 9 to be drawn. It shows the relative effect of different parameters and also illustrates the number of parameters affecting foil selection. One chart requires that the following parameters will be fixed: foil series definition (e.g., NACA 16-), aspect ratio, sweep, taper, dihedral, pod size, depth of submergence, operating speed (i.e., cruise speed), and craft gross weight or foil size, and hence depth-chord ratio, i.e., the chart as at present envisaged only applies to one boat. In order to make the chart applicable to other boats for predesign purposes, the effect of varying such items as foil area (i.e., foil loading) on drag, sweep angle, taper ratio, aspect ratio, and depth of submergence on cavitation is shown briefly in this paper.

The foil section will be chosen after an investigation of minimum drag requirements, sea states, and turning requirements. Normally a boat will be drag sensitive, which the "Fresh I" with HYSTAD is not, and so in choosing a foil section minimum drag requirements may override sea-state requirements. In the present case, BuShips stipulated the

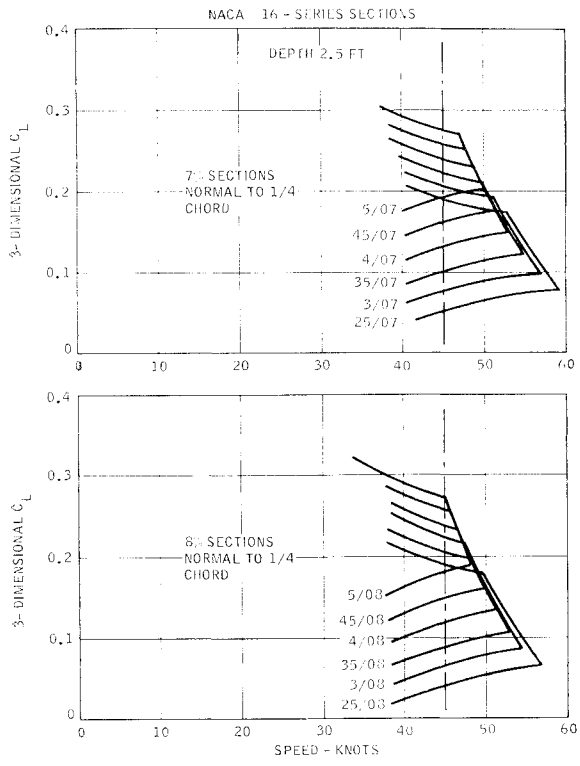

Fig. 8 Factored Abbott buckets.

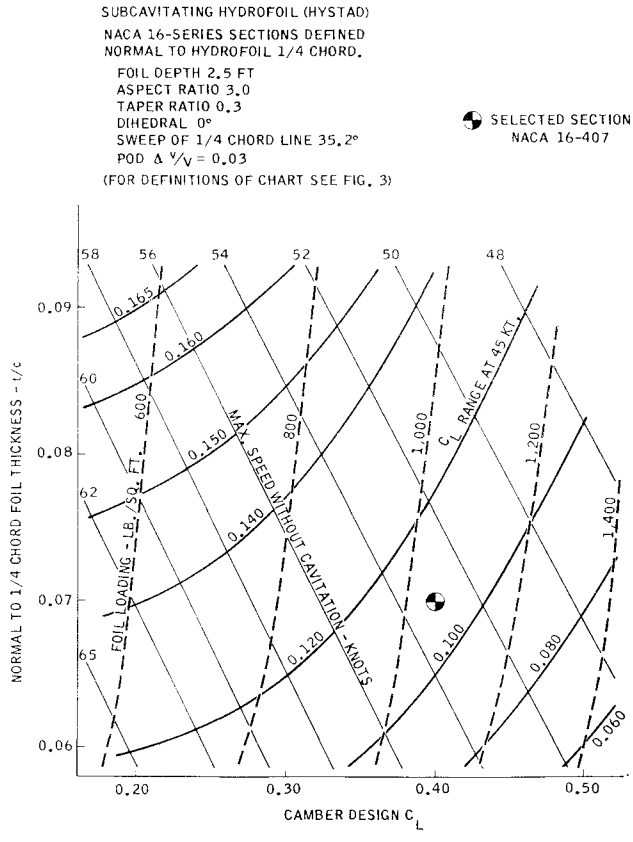

Fig. 9 Foil selection chart.

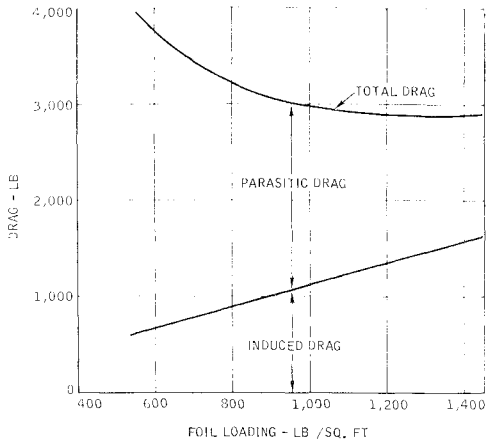

Fig. 10 Foil drag vs foil loading at 45 knots.

requirement that foil loading should be held within normally accepted limits for hydrofoil boats.

Choice of the Foil Section from Consideration of Drag, Sea States, and Turning Characteristics

Drag

For a range of foil loadings between 600 and 1400 psf and a craft weight of 42,000 lb, calculations have been made of the parasitic and induced foil drags, and these have been plotted in Fig. 10. It can be seen that, from a foil drag point of view, the optimum loading is around 1200 psf at 45 knots.

Sea States

Sea-state capability is estimated at the cruise speed of 45 knots, and in the calculations it is assumed that there must be no cavitation beyond the incipient boundary. Foil angles of attack induced by waves in a given sea state[7] and for various craft speeds were obtained for a foil depth of 3 ft.

At 45 knots in a sea state of 2- and 3-ft depth, the root-mean-square value of angle of attack due to waves is 0.685:

$$\tfrac{1}{10}\text{ highest } \alpha = 1.8 \times 0.685 = 1.23°$$

$$\text{total angle of attack range} = 2.46°$$

The three-dimensional C_{L_α} will be about 0.048/deg, and so this represents a C_L range of about 0.12

$$\tfrac{1}{3}\text{ highest } \alpha = 1.42 \times 0.685 = 0.97°$$

total angle of attack range = 2°, giving a C_L range of 0.096

Considering now a sea state of 3 at 45 knots and a 3-ft depth, the root-mean-square value of angle of attack due to waves is 1.10

$$\tfrac{1}{3}\text{ highest } \alpha = 1.42 \times 1.10 = 1.56°$$

total angle of attack range = 3.12°, giving a C_L range of 0.15

For the NACA 16-407 section with Hystad planform, the C_L range uncavitated at 45 knots has been calculated to be 0.11.

It is possible that the craft could run at 45 knots in a sea state of 3 if a small amount of cavitation is accepted. It should be emphasized that the cavitation buckets give the estimated boundaries of incipient cavitation only. If there is going to be any cavitation, it would be preferable to have it on the upper foil surface at the leading edge, i.e., at high angles of attack. This would be because there is a slight increase in C_L for a given α under these conditions. Therefore, it was felt that operation should be slightly above the midpoint of the cavitation bucket at 45 knots.

Craft Turning Characteristics

The conditions existing will be taken as follows: craft weight = 41,500 lb and craft speed = 45 knots, where 80% of the load is on the forward foils. The foils are 13.9 ft vertically below the craft center of gravity, and forces normal to a main foil have an arm of 6 ft about the center of gravity:

$$\text{load normal to main foil surfaces} = \frac{33{,}200}{\cos 10°} = 33{,}700 \text{ lb}$$

$$\text{at 45 knots, } C_L = \frac{33{,}700}{0.995 \times 76.05^2 \times 30.48} = 0.192$$

For the NACA 16-407 section defined normal to $\frac{1}{4}$ chord, C_L at center of bucket at 45 knots = 0.185. Bucket width is 0.11 on C_L. Assume that there is an uncavitated C_L of 0.055 down and 0.055 up on a mean C_L of 0.192:

$$\text{maximum restoring moment} = \tfrac{1}{2}\Delta C_L \rho V^2 S \times 6$$

$$= 0.995 \times 0.11 \times 76.05^2 \times 15.24 \times 6$$

$$= 58{,}000 \text{ lb-ft}$$

$$\text{maximum overturning moment} = (g \text{ factor}) \times 41{,}500 \times 13.9$$

$$(g \text{ factor}) = 58{,}000/577{,}000 = 0.1005$$

i.e., the craft can only stand a 0.1-g flat turn without cavitation at 45 knots:

Centrifugal force 4150	$= Wv^2/gr$ $= (41{,}500/32.2) \times (76.05^2/r)$
Radius of turn r	= 1800 ft
Number of seconds for a 360° turn	= 149
Turning rate	= 2.42 deg/sec

In Fig. 11, the turning radii and turning rates for the craft in a 0.1-g flat turn have been plotted for craft speeds between

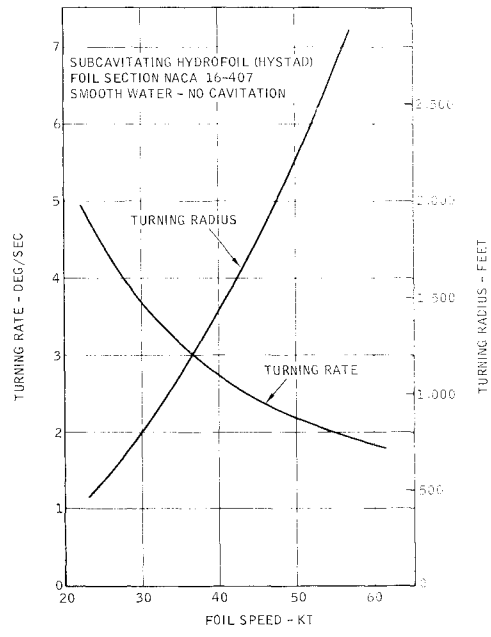

Fig. 11 Turning performance in a 0.1-g flat turn.

Table 2 Results from BuShips method of analysis: three-dimensional cavitation data for "HYSTAD" main foil at an operating depth of 2.5 ft (body $\Delta v/V$ 0.03, NACA 16-308)

Av., C_L	Sheared region, 75% span C_L[a]	Sheared region, 75% span $C_{K_{crit}}$	Sheared region, adj. kink C_L[b]	Sheared region, adj. kink $V_{K_{crit}}$	Kink region C_L[c]	Kink region $C_{K_{crit}}$
−0.03	−0.0372	22.3[d]	−0.0335	22.8	...	...
0.00	0.0000	27.0	0.0000	27.0[d]	...	...
0.03	0.0372	34.0	0.0335	32.8[d]	...	...
0.07	0.0870	55.5	0.0783	49.4[d]	0.0669	53.6
0.10	0.1241	62.9	0.1118	63.3	0.0956	52.3[d]
0.12	0.1490	62.0	0.1342	62.5	0.1147	51.5[d]
0.15	0.1861	60.7	0.1677	61.3	0.1434	50.4[d]
0.18	0.2235	52.0	0.2012	59.2	0.1721	49.4[d]
0.20	0.2482	45.6[d]	0.2236	51.9	0.1912	48.7
0.22	0.2733	40.2[d]	0.2460	46.0	0.2103	48.0
0.24	0.2980	35.4[d]	0.2683	41.1	0.2294	...
0.26	0.3228	31.5[d]	0.2907	36.3	0.2486	...
0.30	0.3723	25.8[d]	0.3354	...	0.2868	...
0.35	0.4345	20.5[d]	0.3913	...	0.3346	...

[a] Factor 1.241.
Factor 1.118.
[c] Factor 0.956.
[d] Critical velocity.

25 and 55 knots. It should be noted that a flat turn is an unusual condition. Most turns will be coordinated turns, i.e., where the pilot applies a certain amount of bank by means of ailerons. In this case, much smaller turning radii could be achieved without overloading the outer foil.

In choosing the NACA 16-407 foil section for the "Fresh I" with Hystad, a compromise was reached between the conditions imposed by drag, sea states, and turning. A foil section giving a wider bucket than the 407 would have been capable of operation in higher sea states and have had better turning characteristics, but its allowable loading would have been lower, meaning larger foil areas, and its drag would have been higher. Although "Fresh I" has a large excess of thrust for a subcavitating system, it was not intended that the Hystad version should depart far from the normally accepted foil loadings for existing hydrofoil boats.

Foil Cavitation Characteristics by the BuShips Method

The method outlined by Johnson[3] was used, with assistance given by Code 420 of BuShips. It involved the use of five computer programs, three of which were forwarded to General Dynamics by BuShips for use on the IBM 1620 computer. The five computer programs are as follows:

1) RSJ-080 is used for calculating the Abbott buckets in the "kink" region. This program was also used in the preparation of the foil selection chart, which is described earlier in this paper.

2) WDB 103-Z is used for calculation of the spanwise lift by the lifting line theory for a given foil planform.

3) WDB/MRH 094 is used to prepare the data for the IBM 7090 program DTMB 840-041.

4) DTMB 840-041 is used for calculation of the two-dimensional pressure distributions by the Brockett method.

5) WDB 091 is the program which gives section ordinates for the Loft lines.

The greatly abbreviated exercise given here will be for the development of the cavitation characteristics of the NACA 16-308 section. The "kink" calculations have been performed for two limiting values of pod $\Delta v/V$ but at only one depth. The depth chosen was 2.5 ft, as this is applicable to the high-speed case. The two-dimensional swept Brockett buckets for the sheared region were calculated for three water depths between 2.5 and 8 ft. The "sheared region adjacent to the kink" was taken as 30% of the semispan from the pod centerline, and the "kink" region as immediately adjacent to the pod.

The following factors were used as in the Johnson report (Ref. 3, p. 43):

$$C_{L_{\alpha \text{ exp. } 2\pi}} = 0.92$$

$$\frac{\alpha_{L=0 \text{ exp.}}}{\alpha_{L=0 \text{ theor.}}} = 0.70$$

Figure 12 shows the two-dimensional Brockett cavitation buckets for three water depths for the NACA-16-308 section with the Abbott "kink" buckets overlaid.

The factors for obtaining the equivalent Table B-2 of Johnson's report are obtained from the results for the spanwise lift distribution: (computer program WDB 103 Z). These factors are as follows for the primary main foil of the subcavitating hydrofoil (Hystad) at a foil depth of 2.5 ft.

Sheared region:

$$\frac{C_{L_{\alpha \text{ local}}}}{C_{L_{\alpha \text{ av}}}} = 1.241$$

Sheared region adjacent to kink:

$$\frac{C_{L_{\alpha \text{ local}}}}{C_{L_{\alpha \text{ av}}}} = 1.118$$

Kink region:

$$\frac{C_{L_{\alpha \text{ local}}}}{C_{L_{\alpha \text{ av}}}} = 0.956$$

Using these factors and Fig. 12, Table 2 was constructed giving the three-dimensional cavitation bucket for a depth of 2.5 ft and pod $\Delta v/V = 0.03$ for the NACA-16-308 section. This bucket is plotted in Fig. 7.

Calculation of Two-Dimensional Cavitation Buckets by the Abbott Method

In this procedure,[6] chordwise pressure distributions are calculated to obtain V_C for a range of angles of attack, using the two-dimensional wind tunnel C_L vs α curve for the appropriate NACA 16-series section.[8] The pressure coefficient C_p at any α can then be computed by the equation

$$\left(\frac{C_{pU}}{C_{pL}}\right) = \frac{\Delta p}{q} = 1 - \left[\frac{v}{V} \pm \frac{\Delta v}{V} \pm \frac{\Delta v_a}{V}\right]^2$$

where the plus signs on the right are used when computing C_{pU}, and the minus signs are used when computing C_{pL}. The cavitation inception velocity V_C for a given α is then deter-

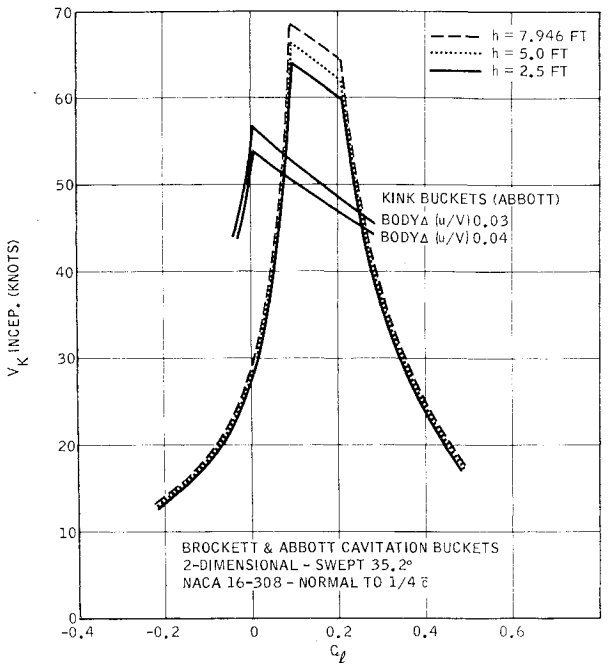

Fig. 12 Foil evaluation by BuShips method.

mined by picking off the pressure plot, the maximum negative pressure, and then substituting it into the formula for critical cavitation speed:

$$V_C = \left(\frac{p_\infty - p_v}{\frac{1}{2}\rho(-\Delta p/q)}\right)^{1/2} \text{fps}$$

This calculation can be performed quite rapidly by hand, but the use of the computer program RSJ-080 enables a larger number of sections to be evaluated. A total of 36 sections were evaluated in the preparation of the foil selection chart, including the six sections used in the BuShips detailed approach. Table 1 shows typical results from the RSJ-080 program for the NACA 16-273/0727 streamwise section (NACA 16-308 section normal to $\frac{1}{4}$ chord with wing taper taken into account) with three-dimensional factoring of C_L and critical velocity.

Effect of Various Parameters on the Three-Dimensional Cavitation Buckets

Depth of Submergence

In the BuShips detailed calculations for the three-dimensional cavitation buckets, the main effect of depth is that of change of static pressure at the foil. For the calculation of cavitation speed in the "kink" region by the Abbott method,

$$V_C = \left(\frac{p_\infty - p_v}{\frac{1}{2}\rho(-\Delta p/q)}\right)^{1/2} \text{fps}$$

for 8-ft depth $(p_\infty - p_v) = 2593$ psf, and for 2.5-ft depth $(p_\infty - p_v) = 2241$ psf. In the same way, depth of submergence comes into the calculation of two-dimensional cavitation velocities for the Brockett buckets. The results of the D.T.M.B. computer program give $(-\Delta p/q)$.

Depth/chord ratio comes into the results for spanwise lift distribution and hence into the factors for the final Table 2. (Johnson[3] states that, after the lifting line theory calculations were completed and the spanwise variation of the lift curve slope was obtained, a free surface correction was applied.) A further effect comes into the "kink" region in the value of $\Delta v/V$ to be taken for the pod.

The depth correction in the foil lift calculations is from Wadlin.[9] This reference provides an approximate solution for the finite depth, rectangular planform unswept foil. The results are given as a ratio of the lift-curve slope at finite depth divided by the lift-curve slope at infinite depth, as a function of depth-chord ratio h/c and aspect ratio A.

Figure 13 shows the effect of going from 2.5-ft depth to 8-ft depth with the NACA 16-308 section defined normal to $\frac{1}{4}$ chord. It can be seen that the bucket is not only widened considerably with the mean C_L staying about the same, but the bottom of the bucket also is carried out to a higher craft speed.

Sweep Angle of $\frac{1}{4}$ Chord Line

The freestream speed for the swept wing V_s is increased by a factor of $1/\cos\Lambda$ over the freestream speed of the straight wing for equal hydrodynamic forces, i.e.,

$$V_s = V/\cos\Lambda \qquad q_s = q/\cos^2\Lambda$$

since, by definition,

$$C_L = L/qS \qquad C_{LS} = C_L \cos^2\Lambda$$

These factors have been applied to the C_L vs speed plot for the NACA 16-407 section defined for a normal to quarter chord sweep of 35.2°. Cavitation buckets have been obtained for sweep angles of 0°, 15°, 30°, and 45° and are plotted in Fig. 14. As sweep is increased, its effects become progressively more rapid, as expected. Three-dimensionally, the effects may not be quite so pronounced. In air, both velocity and critical Mach number are functions of minimum pressure coefficient. Perkins and Hage[10] state that two-dimensionally $M_{CRS} = M_{CR}/\cos\Lambda$, as in the case of freestream speed, but three-dimensional test data on swept back wings indicate that the critical Mach number is increased over a straight wing by a factor of approximately $1/(\cos\Lambda)^{1/2}$, i.e.,

$$M_{CRS} = M_{CR}/\cos\Lambda)^{1/2}$$

Taper Ratio

Bauman,[5] in Fig. A-1 of his report, gives a plot of span factor vs taper ratio which he states is applicable between foil areas of 22 and 55 ft², sweep angles between 10° and 35°, and aspect ratios between 2 and 6. The depth is 4 ft, and the load on his main foils is 20.9 tons, giving foil loadings between 960 and 2400 psf:

$$\text{span factor} = k = C_{l_{\alpha\,\max}}/C_{l\alpha}$$

The effect of planform on the two-dimensional cavitation bucket is essentially to reduce the C_L range by k, i.e., the

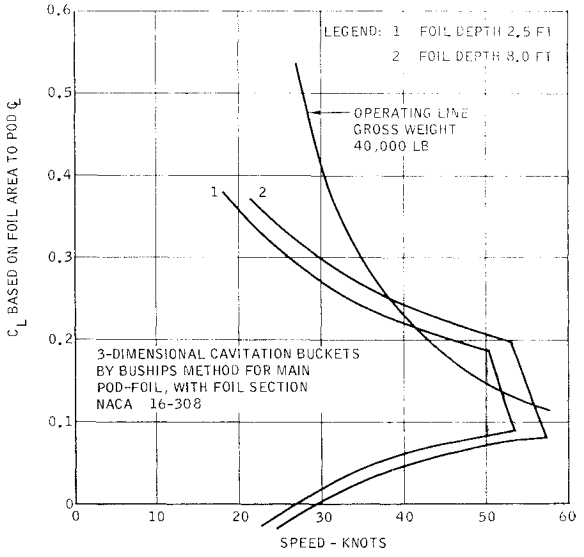

Fig. 13 Effect of depth on cavitation.

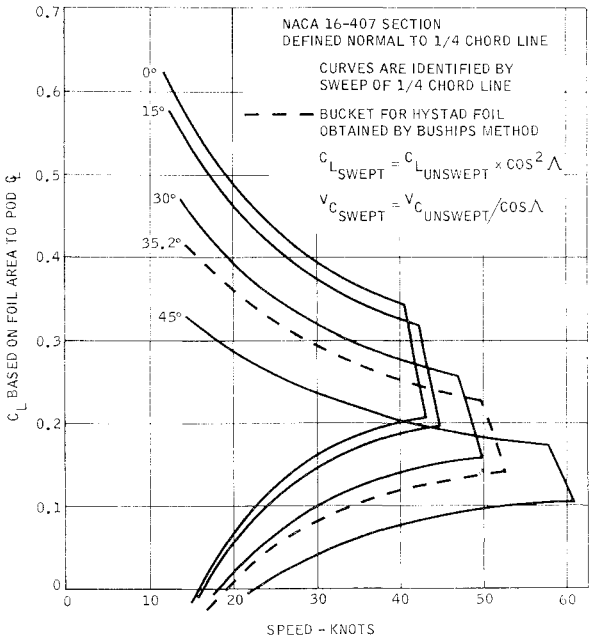

Fig. 14 Effect of sweep on cavitation.

bucket is narrowed. The span factor is primarily a function of taper ratio for a given depth. Foil area, aspect ratio, and sweep provide only a small contribution to span factor.

Bauman used the following figures with a sweep of 30°: taper ratio = 0.2, 0.3, and 0.4; k = 1.35, 1.22, and 1.16, respectively. Then $\Delta C_{L_{(\text{taper})}} = \Delta C_{L_{(\text{no taper})}}/k$. The sides of the three-dimensional cavitation bucket are obtained by correcting both sides of the two-dimensional Brockett bucket by the span factor. The effect is largest on the positive-angle-of-attack side.

Using the values of k just given, Fig. 15 was plotted showing the effect of variation of taper ratio between 0.2 and 0.4 on the three-dimensional cavitation bucket for the NACA 16-407 section plotted normal to the $\frac{1}{4}$ chord.

Aspect Ratio

Aspect ratio affects spanwise lift distribution slightly, and it also affects the depth correction to a certain extent. It chiefly affects the foil lift curve slope but does not appear to affect cavitation buckets significantly when these are plotted as C_L vs speed. Aspect ratio will be principally governed by foil strength and stiffness considerations.

Conclusions

The problems of designing for cavitation-free operation on hydrofoils are quite complex. It would be desirable to have more experimental data, both model and full-scale, to back up theoretical estimates. The experimental work of Ref. 2, carried out after this present work was completed, indicates that, although the estimated cavitation bucket is centered correctly on the measured bucket, it seems to be conservative on C_L range without cavitation at a given speed and indicates too high a speed at the optimum C_L for flow without cavitation.

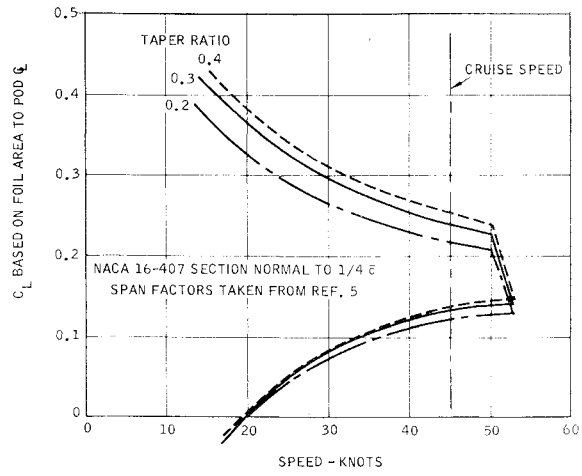

Fig. 15 Effect of taper ratio on cavitation.

It was found that individual analytical estimates must be made of cavitation buckets for both model and full-size foils. The Ref. 2 work, carried out at two depths, showed that cavitation buckets for the same foil at different depths cannot be scaled from full scale to model scale simply by equating cavitation numbers.

The major factors affecting the hydrofoil selection chart in this paper are depth of foil submergence and sweep angle. The chart in this paper is for a depth of 2.5 ft and a fixed mean foil chord of 2.5 ft. Charts should be drawn for other depths, as well as other depth/chord ratios, for various sweep angles, in order to have available a really useful predesign tool.

References

[1] Conolly, A. C., "Towing Basin tests of $\frac{1}{10}$th scale Hystad hydrofoils," Marine Technology Center, General Dynamics, Electric Boat Div., Rept. GD/EB MTC-65-007 (December 1965).

[2] Spangler, P. K., "Model test results for the Hystad strut-nacelle-foil combination," David Taylor Model Basin Rept. 2138 (November 1965).

[3] Johnson, R. S., "Prediction of lift and cavitation characteristics of hydrofoil-strut arrays," Southern California Section, Society of Naval Architects and Marine Engineers (March 19, 1964).

[4] Brockett, T., "Steady two-dimensional pressure distributions on arbitrary profiles," David Taylor Model Basin Rept. 1821 (October 1965).

[5] Bauman, W. D., "A preliminary hydrofoil design incorporating a cavitation-free operation requirement," BuShips Publication (December 1964).

[6] Abbott, I. H., Von Doenhoff, A. E., and Stivers, L. S., Jr., "Summary of airfoil data," NACA Rept. 824 (1945); also *Theory of Wing Sections* (Dover Publications Inc., New York, 1958).

[7] Martin, J. and Turpin, F. J., "The effect of surface waves on some design parameters of a hydrofoil boat," Hydronautics Inc., TR 001-3 (January 1961).

[8] Stack, J., "Tests of airfoils designed to delay the compressibility burble," NACA Rept. 763 (1943).

[9] Wadlin, K. L., Shuford, C. L., Jr., and McGehe, J. R., "A theoretical and experimental investigation of the lift and drag characteristics of hydrofoils at subcritical and supercritical speeds," NACA TR 1232 (April 1952).

[10] Perkins, C. D. and Hage, R. E., *Airplane Performance, Stability, and Control* (John Wiley and Sons Inc., New York, 1960), p. 101.